clinical and translational neuroscience

MDPI

Article

Susceptibility Weighted Imaging as a Biomarker for Cortical Spreading Depression

Adrian Scutelnic, Isabelle Dominique Stöckli, Antonia Klein, Franz Riederer, Nedelina Slavova † and Christoph J. Schankin *,†

Department of Neurology, Inselspital, University Hospital Bern, University of Bern, Freiburgstrasse, CH-3010 Bern, Switzerland; adrian.scutelnic@insel.ch (A.S.); isabelle.stoeckli@students.unibe.ch (I.D.S.); antonia.klein@insel.ch (A.K.); franz.riederer@insel.ch (F.R.); nedelina.slavova@insel.ch (N.S.)

* Correspondence: christoph.schankin@insel.ch

† These authors contributed equally to this work.

Abstract: Introduction: Cortical spreading depression (CSD) is thought to be the pathophysiologic correlate of migraine aura. In experimental animals, CSD was shown to cause an increase in oxyhemoglobin. Susceptibility weighted imaging (SWI) on magnetic resonance imaging (MRI) depicts cerebral veins according to their concentration in oxyhemoglobin. The aim of this study was to assess whether the distribution of SWI changes in people with migraine aura resembles the clinical presentation, with a focus on topology. Methods: In this retrospective single-center study, patients were included if they (i) had acute focal neurological symptoms beginning with visual symptoms, (ii) underwent head MRI including SWI within eight hours of symptom onset, (iii) SWI showed focal dilated veins, and (iv) they had a discharge diagnosis of migraine with aura. Eleven predefined cerebral regions of interest (ROIs) were assessed for prominent focal veins (PFVs) on SWI. We determined whether symptoms correlated with the topography of ROIs with PFVs. Results: We found a posterior to anterior gradient of SWI changes during acute migraine aura when visual symptoms were present. Conclusion: MRI with SWI might be able to detect traces of CSD. The posterior to anterior distribution of areas with SWI changes corresponds anatomically to the canonical succession of symptoms in migraine aura.

Keywords: cortical spreading depression; migraine with aura; susceptibility weighted imaging; cerebral veins

Academic Editor: Jian Wang

Received: 26 November 2024
Revised: 30 December 2024
Accepted: 14 January 2025
Published: 20 January 2025

Citation: Scutelnic, A.; Stöckli, I.D.; Klein, A.; Riederer, F.; Slavova, N.; Schankin, C.J. Susceptibility Weighted Imaging as a Biomarker for Cortical Spreading Depression. *Clin. Transl. Neurosci.* **2025**, *9*, 3. https://doi.org/10.3390/ctn9010003

1. Introduction

After Leão's first description of cortical spreading depression (CSD) in rabbits in 1944, its presence in the non-injured healthy human brain has only been inferred from a few in vivo techniques [1]. Markers for migraine aura are important in clinical practice and for our understanding of its pathophysiology, given the phenotypical overlap of migraine aura with other differential diagnoses such as vascular lesions or epileptic seizures [2].

The CSD was hypothesized to be the pathophysiologic correlate of migraine aura [3]. Given that migraine aura often contains visual symptoms, it is assumed that the occipital lobes have the highest likelihood of CSD generation, and CSD likely starts in the occipital lobes and slowly spreads rostrally [4,5]. The initial occipital localization of functional changes during migraine aura was demonstrated in three subjects assessing blood oxygenation level-dependent signal changes (BOLD) [5,6]. BOLD is usually available in research settings only. Susceptibility weighted imaging (SWI), in contrast, is part of most routine non-contrast magnetic resonance tomography (MRI) protocols and thus might be of use in

imaging migraine aura. SWI changes during acute migraine aura were present in two-thirds of a large population of pediatric patients [7]. In his original description of CSD, Leão found an increase in oxyhemoglobin in pial veins following a wave of CSD [1]. However, whether oxyhemoglobin has a specific role during a migraine attack or is simply a consequence of CSD is not known. SWI depicts the cerebral veins according to their concentration in oxyhemoglobin [8]. We therefore hypothesize that the SWI might be a marker for CSD.

The aim of this study was to assess whether the distribution of SWI changes in people with migraine aura resemble the clinical presentation with a focus on topology.

2. Methods

This is a single-center retrospective cohort study. Study population consisted of patients presenting at the emergency department of Inselspital Bern. The inclusion criteria were (i) acute focal neurological symptoms beginning with visual symptoms; (ii) the patients underwent a head MRI, including susceptibility weighted sequences (SWI), within eight hours of symptom onset to exclude secondary causes, such as stroke or other structural findings; (iii) SWI showed focal dilated veins; and (iv) a discharge diagnosis of migraine with aura was made after all clinical data were taken into account. Patients with other co-morbidities (e.g., psychiatric, vascular risk factors) were not excluded. In addition, we exploratorily tested the hypothesis of whether the posterior regions are always involved in migraine aura by identifying patients without visual symptoms.

The inclusion of patients with MRI within eight hours of symptom onset was performed based on a previous study demonstrating persistent SWI changes within this time-frame in migraine with aura [7]. The diagnosis of migraine with aura was made by experienced board-certified neurologists in the emergency setting. The authors further re-assessed the discharge letters to verify diagnoses according to the criteria of The International Classification of Headache Disorders 3rd Edition [9].

Each MRI scan was evaluated by a board-certified neuroradiologist (NS) at three horizontal levels: at the mesencephalon level, the basal ganglia level and the insula level (Figure 1). The MRI scans were specifically evaluated for SWI changes at a later timepoint than the presentation at the emergency department. A total of 10 regions per hemisphere were defined. The first slice from inferior to superior is based on the level of the mesencephalon and includes the regions P1 (occipital inferior) and M1 (temporal inferior). The second slice at the level of the basal ganglia includes P2 (occipital superior), M2p (temporal superior), M2a (temporal opercular) and A1 (frontal inferior). The last slice parallels the ventricles above the insula and includes P3 (parietal), M3 (frontoparietal excluding MC), MC (motor cortex, central) and A2 (frontal superior).

We then analyzed each of the 11 brain regions for SWI changes. Each region was scored according to whether prominent focal veins (PFVs) could be seen and classified accordingly as with or without PFVs. For the analysis, several regions of interest (ROIs) were then merged, i.e., handled as subgroups that anatomically corresponded to corresponding symptoms (in order from posterior to anterior); the regions P1, P2, and P3 corresponded to visual symptoms and were named collectively area P; the regions M1 and M2p corresponded to sensory symptoms and were named area Mp; the regions M2a and M3 corresponded to aphasia and dysarthria and were named area Ma; the region MC was named area MC and corresponded to motor disturbance; and finally, the regions A1 and A2 were named collectively area A. Once a ROI within an area had SWI changes, the whole area was considered as having SWI changes regardless of whether there was PFVs in only one or all ROIs of that area.

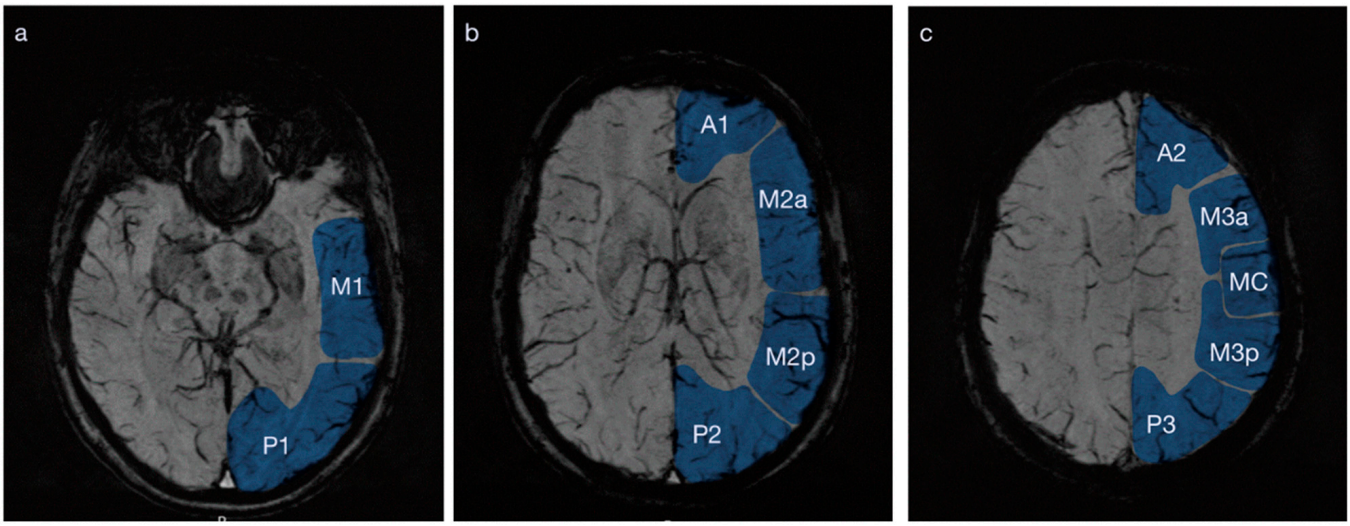

Figure 1. Three axial MR SWI slices, arranged from inferior to superior, at the level of (**a**) the mesencephalon, (**b**) the basal ganglia and (**c**) the centrum semiovale just above the lateral ventricles. P1 = occipital inferior, M1 = temporal inferior; P2 = occipital superior, M2p = temporal superior, M2a = temporal opercular, A1 = frontal inferior; P3 = parietal, M3p and M3a = frontoparietal excluding MC (divided into posterior and anterior sections), MC = motor cortex, central, A2 = frontal superior.

We further analyzed concomitantly and contiguously affected areas in three planes for the left and right hemisphere separately: at the mesencephalon plane (P1 + M1), at the basal ganglia plane (P2 + M2p, P2 + M2p + M2a, and P2 + M2p + M2a + A1) and above the lateral ventricles (P3 + M2p, P3 + M2p + Mc, P3 + M2p + Mc + M2a, and P3 + M2p + Mc + M2a + A2).

In the subjects without visual symptoms, we assessed SWI changes in the P1, P2 and P3 regions to approximate specificity of the SWI changes.

3. Results

In all, 18 patients were included in this study. Ten (56%) were women and the median age was 32 (interquartile range [IQR] 29–59). The MRI was performed after a median of 205 min (IQR 157–352) after aura onset. Overall, 18/18 (100%) patients had visual symptoms, 10/18 (56%) had sensory symptoms, 12/18 (67%) had speech disturbance, and 3/18 (17%) had motor symptoms.

All 18 patients with visual disturbances had SWI changes in the posterior region (details visualized in Figure 2). Of the 12 patients with speech disturbance, all 12 had SWI-changes in the Ma region, 5/12 (42%) had changes in the A region and none had changes in the MC region. Of the 10 patients with sensory disturbance, all had changes in the M region, 6 (60%) had changes in the A region and 2 (20%) had changes in the MC region. Of the three patients with motor symptoms, all patients had changes in the M region, two (67%) had changes in the A region and one (33%) had changes in the MC region. The distribution of symptoms for each region is given in Table 1.

With each added area with PFVs, the proportions of affected patients declined (see Table 2), e.g., for patients with visual symptoms with PFVs in the left hemisphere, there were 10/12 (56%) with PFVs in the P2 + M2p areas, 7/12 (59%) in the P2 + M2p + M2a and 2/12 (11%) in the P2 + M2p + M2a + A1 areas. This pattern of distribution was observed for all symptoms and both hemispheres.

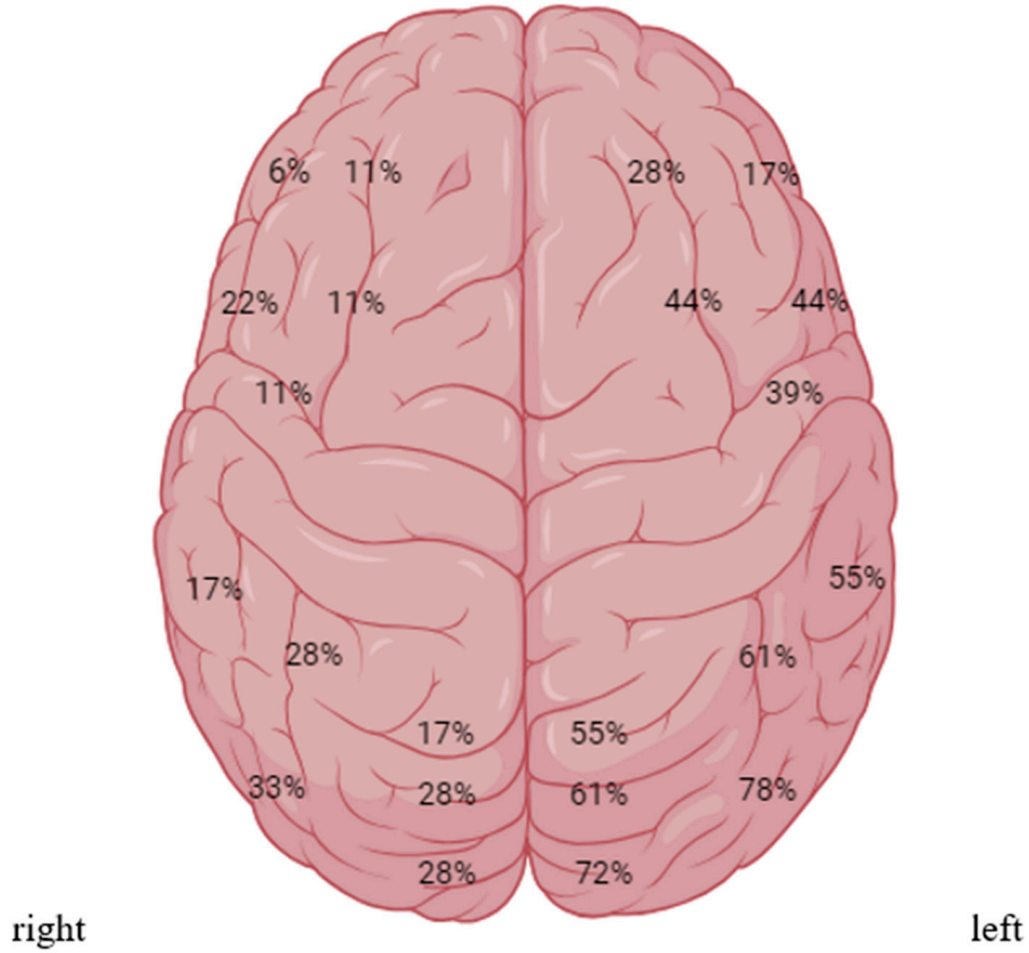

Figure 2. Distribution of susceptibility weighted imaging (SWI) changes (created in BioRender.com). The percentages depict the frequencies of the SWI changes during acute migraine aura. The SWI changes were more frequent in the posterior regions, with a clear posterior to anterior gradient. There was a left-hemispheric dominance, likely due to a selection of patients with left-hemispheric symptoms, which, being more severe (e.g., aphasia), are more likely to be worked-up in the emergency setting.

Looking at the association between lack of symptoms (e.g., sensory) and PFVs, there were frequent changes in eloquent areas despite patients reporting no symptoms corresponding to the affected area (Table 3).

We identified additional 10 patients without visual symptoms. Of these, only 5/10 (50%) had SWI changes in at least one of the posterior regions P1, P2 and/or P3.

Table 1. Distribution of affected areas by symptoms.

	Visual, N = 18,	**Left Hemisphere**	**Right Hemisphere**	**Sensory, N = 10**	**Left Hemisphere**	**Right Hemisphere**	**Speech, N = 12**	**Left Hemisphere**	**Right Hemisphere**	**Motor, N = 3**	**Left Hemisphere**	**Right Hemisphere**
P1 [1], n/N (%)	17 (94)	13 (72)	5 (28)	9 (90) [1]	5 (50)	4 (40)	11 (92)	11 (92)	1 (8)	2 (67)	1 (33)	1 (33)
P2 [2], n/N (%)	14 (78)	11 (61)	5 (28)	10 (100) [1]	5 (50)	4 (40)	10 (83)	10 (83)	1 (8)	2 (67)	1 (33)	1 (33)
P3, n/N (%)	13 (72)	10 (56)	3 (17)	9 (90)	6 (60)	3 (30)	10 (83)	9 (75)	1 (8)	3 (100)	2 (67)	1 (33)
M1, n/N (%)	14 (78)	11 (61)	3 (17)	8 (80)	5 (50)	3 (30)	12 (100)	11 (92)	1 (8)	2 (67)	1 (33)	1 (33)
M2p [3], n/N (%)	17 (94)	14 (78)	6 (33)	10 (100)	7 (70)	5 (50)	12 (100)	11 (92)	3 (25)	3 (100)	3 (100)	1 (33)
M3p [1], n/N (%)	15 (83)	11 (61)	5 (28)	9 (90)	5 (50)	5 (50)	8 (67)	9 (75)	2 (17)	3 (100)	2 (67)	2 (67)
M3a, n/N (%)	10 (56)	8 (44)	2 (11)	8 (80)	6 (60)	2 (20)	7 (70)	6 (50)	1 (10)	3 (100)	2 (67)	1 (33)
M2a, n/N (%)	12 (67)	8 (44)	4 (22)	7 (70)	4 (40)	3 (30)	10 (83)	8 (67)	2 (17)	2 (67)	1 (33)	1 (33)
MC, n/N (%)	9 (50)	7 (39)	2 (11)	7 (70)	5 (50)	2 (20)	6 (50)	6 (50)	0	3 (100)	2 (67)	1 (33)
A1, n/N (%)	4 (22)	3 (17)	1 (6)	3 (30)	2 (20)	1 (10)	3 (25)	3 (25)	0	1 (33)	1 (33)	0
A2, n/N (%)	7 (39)	2 (11)	5 (28)	6 (60)	4 (40)	2 (20)	5 (42)	5 (42)	0	2 (67)	1 (33)	1 (33)

[1] in n = 1 bilateral changes, [2] in n = 2 bilateral changes, [3] in n = 3 bilateral changes.

Table 2. Distribution of affected overlapping areas by type of symptoms.

	Visual, N = 18		**Sensory, N = 10**		**Speech, N = 12**		**Motor, N = 3**	
	Left Hemisphere	**Right Hemisphere**	**Left Hemisphere**	**Right Hemisphere**	**Left Hemisphere**	**Right Hemisphere**	**Left Hemisphere**	**Right Hemisphere**
The Mesencephalon Level								
P1 + M1, n/N (%)	11 (61)	3 (17)	5 (50)	3 (30)	11 (92)	1 (8)	1 (33)	1 (33)
The basal ganglia level								
P2 + M2p, n/N (%)	10 (56)	4 (22)	5 (50)	4 (40)	10 (83)	1 (8)	1 (33)	1 (33)
P2 + M2p + M2a, n/N (%)	7 (39)	3 (17)	4 (40)	3 (30)	7 (58)	1 (8)	1 (33)	1 (33)
P2 + M2p + M2a + A1, n/N (%)	2 (11)	1 (6)	2 (20)	1 (10)	2 (17)	0	1 (33)	0
The ventricular level								
P3 + M3p, n/N (%)	9 (50)	3 (17)	5 (50)	3 (30)	7 (58)	2 (17)	2 (67)	1 (33)
P3 + M3p + Mc, n/N (%)	6 (33)	2 (11)	4 (40)	2 (20)	5 (42)	1 (8)	2 (67)	1 (33)
P3 + M3p + Mc + M3a, n/N (%)	5 (28)	2 (11)	4 (40)	2 (20)	4 (33)	1 (8)	2 (67)	1 (33)
P3 + M3p + Mc + M3a + A2, n/N (%)	3 (17)	2 (11)	3 (30)	2 (20)	3 (25)	1 (8)	1 (33)	1 (33)

Table 3. Distribution of areas with prominent focal veins in patients with absent symptoms despite SWI changes in eloquent regions.

		No Sensory Symptoms, N = 8		**No Speech Disturbance, N = 6**		**No Motor Symptoms, N = 15**	
		Left Hemisphere	**Right Hemisphere**	**Left Hemisphere**	**Right Hemisphere**	**Left Hemisphere**	**Right Hemisphere**
P region	P1, n/N (%)	8 (100)	1 (13)	2 (33)	4 (67)	12 (80)	4 (27)
	P2, n/N (%)	6 (75)	1 (13)	1 (17)	4 (67)	10 (67)	4 (27)
	P3, n/N (%)	4 (50)	0	1 (17)	2 (33)	8 (53)	2 (13)
Mp region	M1, n/N (%)	6 (75)	0	0	2 (33)	10 (67)	2 (13)
	M2p, n/N (%)	7 (88)	1 (13)	3 (50)	3 (50)	11 (73)	5 (33)
	M3p, n/N (%)	6 (75)	0	2 (33)	1 (17)	8 (53)	5 (33)
Ma region	M3a, n/N (%)	2 ()	0	2 (33)	1 (17)	6 (40)	1 (7)
	M2a, n/N (%)	4 (50)	1 (13)	0	2 (33)	7 (47)	3 (20)
Mc region	MC, n/N (%)	2 (25)	0	1 (17)	2 (33)	5 (33)	1 (7)
A region	A1, n/N (%)	1 (13)	0	0	1 (17)	2 (13)	1 (7)
	A2, n/N (%)	1 (13)	0	0	2 (33)	4 (27)	1 (7)

4. Discussion

The main findings of our study is the posterior to anterior gradient of SWI changes during acute migraine aura, when visual symptoms are present. This supports the hypothesis that SWI changes might be an imaging marker for CSD. One hypothesis explaining the emergence of CSD in the posterior regions is likely related to the histological composition of the posterior regions. In human and monkeys, it was shown that the posterior regions have a higher density of neurons compared to the anterior regions. Since the CSD is a neuronal phenomenon that is inhibited by astroglial cells, which have a higher density in the anterior regions of the cortex, it is more likely that the CSD originates in the posterior regions [5,6,10–12]. Furthermore, in females with migraine aura the cortical thickness in the occipital regions was higher than in females without migraine [13]. In addition, the vasomotor autoregulation was impaired in patients with migraine aura, possibly explaining the increase in deoxyhemoglobine during an attack [14–24]. In contrast to more sophisticated laboratory [25] but also imaging methods, such as BOLD and machine learning algorithms, MRI-SWI is widely available [26,27].

However, there are some unclear aspects related to our findings. First, it is not clear why some regions had PFV despite the patients not reporting symptoms corresponding to the affected areas. This was also the case for the posterior region in people without visual symptoms of migraine aura. The phenomenon of silent CSD has been proposed, which is a CSD wave spreading thorough a non-eloquent brain area, which does not have a subjectively perceived function [28]. On the other hand, this might also be caused by the reporting and/or assessment bias in an emergency setting, and further prospective studies are needed to confirm or infirm this finding. Furthermore, we cannot know for sure whether the regions of interest we chose correspond to an anatomical function given their large distribution. Our qualitative (and not quantitative) assessment might have biased our analyses of SWI changes related to the presence or absence of symptoms.

Second, looking at patients with no visual symptoms, there was, as mentioned, still a proportion with changes in the posterior regions. In addition to this possibly being explained by silent auras, the presence of PFV in only 50% compared to 100% in auras with visual symptoms supports that SWI changes are indeed associated with CSD and might be a marker of migraine aura, as hypothesized for this study based on SWI depicting veins according to their content of deoxyhemoglobin and Leão showing an increase in deoxyhemoglobin after a wave of CSD [1,8,29]. Furthermore, the posterior to anterior distribution of the SWI changes we found in our study corresponds to the usual succession of symptoms in migraine aura [4]. Therefore, MRI with SWI might be a good method for detecting traces of CSD. The main advantage over more sophisticated methods is that it is widely available and is usually part of standardized MRI protocols in many centers. This is important because migraine aura in its acute phase is very difficult to examine, given its lack of predictability and logistical difficulties related to more advanced imaging techniques. However, its main disadvantage is the low sensitivity, as shown in previous studies [30].

We observed SWI changes localized in regions distal to the central sulcus, which does not correspond to the current theory of CSD, which is thought to cease at anatomical barriers such as big cerebral sulci. This is supported by the clinical observation that true motor weakness, represented in the precentral gyrus, is exceptional in migraine aura, except for the special case of familial hemiplegic migraine. One possible explanation is that the CSD wave travels beyond the central sulcus but loses its ability to cause cerebral dysfunction. This, however, is speculative.

Our study has limitations, with the first and most important one being its retrospective design, with no prospective assessment of symptoms. Furthermore, there were different

protocols of the MRI with different field strengths (1.5T or 3T) and different slice thicknesses. Different MRI protocols might have altered the sensitivity of the results. However, given the consistent findings in this study, we believe that this limitation does not affect our conclusions. Given that the patients were included in an emergency setting, the majority had left-hemispheric symptoms and, therefore, there might have been a selection bias in our study. This is, however, expected, as dysfunction of the left hemisphere causes symptoms that are more worrisome (e.g., speech disturbance). One further limitation is that SWI changes might be affected by vasoactive medication or co-morbidities that might affect blood oxygenation (see Supplemental Table S1 for vascular risk factors, co-morbidities and concomitant medication), which we did not account for. The value of SWI changes in differentiating between migraine aura and other differential diagnoses (e.g., transient ischemic attacks) could not be addressed in this study. Therefore, future case–control adequately powered studies are necessary to address this question. Lastly, the small sample size does not allow for firm conclusions.

In conclusion, MRI with SWI might be used for imaging of CSD. The posterior to anterior distribution of areas with SWI changes corresponds anatomically to the canonical succession of symptoms in migraine aura, suggesting that the CSD might cause the migraine aura. Given the wide availability, MRI with SWI might be used as an imaging marker for migraine aura. We propose investigating the use of SWI in detecting traces of CSD in larger prospective studies using high-field MRI.

Supplementary Materials: The following supporting information can be downloaded at: https://www.mdpi.com/article/10.3390/ctn9010003/s1, Table S1: Vascular risk factors, co-morbidities and medication.

Author Contributions: Conceptualization, C.J.S., N.S., I.D.S. and A.S.; methodology, C.J.S., N.S. and I.D.S.; software, A.S.; validation, C.J.S., N.S., I.D.S., A.S., A.K. and F.R.; formal analysis, A.S., I.D.S. and C.J.S.; investigation, C.J.S., I.D.S., N.S. and C.J.S.; resources, C.J.S.; data curation, A.S., I.D.S., N.S. and C.J.S.; writing—original draft preparation A.S., I.D.S. and C.J.S.; writing—review and editing, all authors.; visualization, A.S., I.D.S., N.S., C.J.S.; supervision, A.S., N.S. and C.J.S.; project administration, A.S. and C.J.S.; funding acquisition, N/A. All authors have read and agreed to the published version of the manuscript.

Funding: This research received no external funding.

Institutional Review Board Statement: This study was approved by the Bern cantonal ethics committee (KEK 2020-00115).

Informed Consent Statement: All included patients signed a general consent for their clinical-related data to be used in anonymized form for research purposes, according to the local regulations.

Data Availability Statement: Upon reasonable request to the corresponding author, original data will be made available.

Conflicts of Interest: The authors declare no conflicts of interest related to this manuscript.

References

1. Leao, A.A. Further observations on the spreading depression of activity in the cerebral cortex. *J. Neurophysiol.* **1947**, *10*, 409–414. [CrossRef]
2. Scutelnic, A.; Petroulia, V.; Schraml, L.; Jung, S.; Branca, M.; Beyeler, M.; Fischer, U.; Wiest, R.; Slavova, N.; Schankin, C.J. The "index vein" as a sign for migraine aura in the emergency setting. *Cephalalgia* **2023**, *43*, 3331024221132010. [CrossRef]
3. O'Hare, L.; Asher, J.M.; Hibbard, P.B. Migraine Visual Aura and Cortical Spreading Depression-Linking Mathematical Models to Empirical Evidence. *Vision* **2021**, *5*, 30. [CrossRef] [PubMed]
4. Scutelnic, A.; Bracher, J.; Kreis, L.A.; Beyeler, M.; Fischer, U.; Arnold, M.; Mattle, H.P.; Jung, S.; Schankin, C.J. Symptoms and patterns of symptom propagation in incipient ischemic stroke and migraine aura. *Front. Hum. Neurosci.* **2023**, *16*, 1077737. [CrossRef]

5. Hadjikhani, N.; Sanchez Del Rio, M.; Wu, O.; Schwartz, D.; Bakker, D.; Fischl, B.; Kwong, K.K.; Cutrer, F.M.; Rosen, B.R.; Tootell, R.B.; et al. Mechanisms of migraine aura revealed by functional MRI in human visual cortex. *Proc. Natl. Acad. Sci. USA* **2001**, *98*, 4687–4692. [CrossRef] [PubMed]
6. Arngrim, N.; Hougaard, A.; Ahmadi, K.; Vestergaard, M.B.; Schytz, H.W.; Amin, F.M.; Larsson, H.B.W.; Olesen, J.; Hoffmann, M.B.; Ashina, M. Heterogenous migraine aura symptoms correlate with visual cortex functional magnetic resonance imaging responses. *Ann. Neurol.* **2017**, *82*, 925–939. [CrossRef]
7. Kellner-Weldon, F.; Lehmann, V.F.; Breiding, P.S.; Grunder, L.; Muri, R.; Pastore-Wapp, M.; Bigi, S.; Wiest, R.; El-Koussy, M.; Slavova, N. Findings in susceptibility weighted imaging in pediatric patients with migraine with aura. *Eur. J. Paediatr. Neurol.* **2020**, *28*, 221–227. [CrossRef]
8. Haacke, E.M.; Xu, Y.; Cheng, Y.C.; Reichenbach, J.R. Susceptibility weighted imaging (SWI). *Magn. Reson. Med.* **2004**, *52*, 612–618. [CrossRef]
9. Headache Classification Committee of the International Headache Society (IHS). The International Classification of Headache Disorders, 3rd edition (beta version). *Cephalalgia* **2013**, *33*, 629–808. [CrossRef] [PubMed]
10. Lauritzen, M.; Dreier, J.P.; Fabricius, M.; Hartings, J.A.; Graf, R.; Strong, A.J. Clinical relevance of cortical spreading depression in neurological disorders: Migraine, malignant stroke, subarachnoid and intracranial hemorrhage, and traumatic brain injury. *J. Cereb. Blood Flow Metab.* **2011**, *31*, 17–35. [CrossRef]
11. Rockel, A.J.; Hiorns, R.W.; Powell, T.P. The basic uniformity in structure of the neocortex. *Brain* **1980**, *103*, 221–244. [CrossRef] [PubMed]
12. Collins, C.E.; Airey, D.C.; Young, N.A.; Leitch, D.B.; Kaas, J.H. Neuron densities vary across and within cortical areas in primates. *Proc. Natl. Acad. Sci. USA* **2010**, *107*, 15927–15932. [CrossRef]
13. Gaist, D.; Hougaard, A.; Garde, E.; Reislev, N.L.; Wiwie, R.; Iversen, P.; Madsen, C.G.; Blaabjerg, M.; Nielsen, H.H.; Krøigård, T.; et al. Migraine with visual aura associated with thicker visual cortex. *Brain* **2018**, *141*, 776–785. [CrossRef] [PubMed]
14. Reinhard, M.; Schork, J.; Allignol, A.; Weiller, C.; Kaube, H. Cerebellar and cerebral autoregulation in migraine. *Stroke* **2012**, *43*, 987–993. [CrossRef] [PubMed]
15. Bäcker, M.; Sander, D.; Hammes, M.G.; Funke, D.; Deppe, M.; Conrad, B.; Tölle, T. Altered cerebrovascular response pattern in interictal migraine during visual stimulation. *Cephalalgia* **2001**, *21*, 611–616. [CrossRef] [PubMed]
16. Lee, M.J.; Cho, S.; Woo, S.Y.; Chung, C.S. Paradoxical association between age and cerebrovascular reactivity in migraine: A cross-sectional study. *J. Neurol. Sci.* **2019**, *398*, 204–209. [CrossRef] [PubMed]
17. Rosengarten, B.; Sperner, J.; Görgen-Pauly, U.; Kaps, M. Cerebrovascular reactivity in adolescents with migraine and tension-type headache during headache-free interval and attack. *Headache* **2003**, *43*, 458–463. [CrossRef]
18. Jiménez Caballero, P.E.; Muñoz Escudero, F. Peripheral endothelial function and arterial stiffness in patients with chronic migraine: A case-control study. *J. Headache Pain* **2013**, *14*, 8. [CrossRef] [PubMed]
19. Vernieri, F.; Moro, L.; Altamura, C.; Palazzo, P.; Incalzi, R.A.; Rossini, P.M.; Pedone, C. Patients with migraine with aura have increased flow mediated dilation. *BMC Neurol.* **2010**, *10*, 18. [CrossRef]
20. Lauritzen, M. Long-lasting reduction of cortical blood flow of the brain after spreading depression with preserved autoregulation and impaired CO_2 response. *J. Cereb. Blood Flow Metab.* **1984**, *4*, 546–554. [CrossRef]
21. González-Quintanilla, V.; Toriello, M.; Palacio, E.; González-Gay, M.A.; Castillo, J.; Montes, S.; Martínez-Nieto, R.; Fernandez, J.; Rojo, A.; Gutiérrez, S.; et al. Systemic and cerebral endothelial dysfunction in chronic migraine. A case-control study with an active comparator. *Cephalalgia* **2016**, *36*, 552–560. [CrossRef] [PubMed]
22. Marouf, W.; Hetzel, A.; Reinhard, M.; Niesen, W.-D. Cerebral ultrasound perfusion imaging in a migraine attack with prolonged aura. *J. Neurol.* **2008**, *255*, 599–600. [CrossRef]
23. Napoli, R.; Guardasole, V.; Zarra, E.; Matarazzo, M.; D'Anna, C.; Saccà, F.; Affuso, F.; Cittadini, A.; Carrieri, P.B.; Saccà, L. Vascular smooth muscle cell dysfunction in patients with migraine. *Neurology* **2009**, *72*, 2111–2114. [CrossRef] [PubMed]
24. Vernieri, F.; Tibuzzi, F.; Pasqualetti, P.; Altamura, C.; Palazzo, P.; Rossini, P.; Silvestrini, M. Increased cerebral vasomotor reactivity in migraine with aura: An autoregulation disorder? A transcranial Doppler and near-infrared spectroscopy study. *Cephalalgia* **2008**, *28*, 689–695. [CrossRef] [PubMed]
25. Dalkara, T.; Kaya, Z.; Erdener, Ş.E. Unraveling the interplay of neuroinflammatory signaling between parenchymal and meningeal cells in migraine headache. *J. Headache Pain* **2024**, *25*, 124. [CrossRef] [PubMed]
26. Mitrović, K.; Savić, A.M.; Radojičić, A.; Daković, M.; Petrušić, I. Machine learning approach for Migraine Aura Complexity Score prediction based on magnetic resonance imaging data. *J. Headache Pain* **2023**, *24*, 169. [CrossRef]
27. Raggi, A.; Leonardi, M.; Arruda, M.; Caponnetto, V.; Castaldo, M.; Coppola, G.; Della Pietra, A.; Fan, X.; Garcia-Azorin, D.; Gazerani, P.; et al. Hallmarks of primary headache: Part 1—Migraine. *J. Headache Pain* **2024**, *25*, 189. [CrossRef]
28. Hansen, J.M.; Baca, S.M.; Vanvalkenburgh, P.; Charles, A. Distinctive anatomical and physiological features of migraine aura revealed by 18 years of recording. *Brain* **2013**, *136 Pt 12*, 3589–3595. [CrossRef]

29. Leao, A.A.P.; Morison, R.S. Propagation of spreading cortical depression. *J. Neurophysiol.* **1945**, *8*, 33–45. [CrossRef]
30. Kellner-Weldon, F.; Jossen, M.; Breiding, P.S.; Grunder, L.; Schankin, C.; Scutelnic, A.; Fischer, U.; Muri, R.; Pastore-Wapp, M.; Wiest, R.; et al. Imaging Neurovascular Uncoupling in Acute Migraine with Aura with Susceptibility Weighted Imaging. *Clin. Neuroradiol.* **2021**, *31*, 581–588. [CrossRef]